doi:10.1093/jmcb/mjy058
Published online November 5, 2018

Article

Acetylation of ACAP4 regulates CCL18-elicited breast cancer cell migration and invasion

Xiaoyu Song[1,3,†], Wei Liu[1,3,†], Xiao Yuan[1,4], Jiying Jiang[1,3], Wanjuan Wang[2], McKay Mullen[3], Xuannv Zhao[1], Yin Zhang[1,2], Fusheng Liu[1,2], Shihao Du[1,2], Adeel Rehman[1], Ruijun Tian[4], Jian Li[3], Andra Frost[5], Zhenwei Song[1], Hadiyah-Nicole Green[3], Calmour Henry[3], Xing Liu[1,3,*], Xia Ding[2,3,*], Dongmei Wang[1,*], and Xuebiao Yao[1,*]

[1] Anhui Key Laboratory for Cellular Dynamics & Chemical Biology, Hefei National Science Center for Physical Sciences at Nanoscale, CAS Center of Excellence in Molecular Cell Sciences, University of Science & Technology of China, Hefei 230027, China
[2] School of Basic Medical Sciences, Beijing University of Chinese Medicine, Beijing 100029, China
[3] Keck Center for Cellular Dynamics & Department of Physiology, Morehouse School of Medicine, Atlanta, GA 30310, USA
[4] Department of Chemistry, Southern University of Science & Technology, Shenzhen 518055, China
[5] Department of Pathology, University of Alabama School of Medicine, Birmingham, AL 35294, USA
[†] These authors contributed equally to this work.
[*] Correspondence to: Xuebiao Yao, E-mail: yaoxb@ustc.edu.cn; Xia Ding, E-mail: dingx@bucm.edu.cn; Dongmei Wang, E-mail: wangdm@ustc.edu.cn; Xing Liu, E-mail: xing1017@ustc.edu.cn

Edited by Jiarui Wu

Tumor metastasis represents the main causes of cancer-related death. Our recent study showed that chemokine CCL18 secreted from tumor-associated macrophages regulates breast tumor metastasis, but the underlying mechanisms remain less clear. Here, we show that ARF6 GTPase-activating protein ACAP4 regulates CCL18-elicited breast cancer cell migration via the acetyltransferase PCAF-mediated acetylation. CCL18 stimulation elicited breast cancer cell migration and invasion via PCAF-dependent acetylation. ACAP4 physically interacts with PCAF and is a cognate substrate of PCAF during CCL18 stimulation. The acetylation site of ACAP4 by PCAF was mapped to Lys311 by mass spectrometric analyses. Importantly, dynamic acetylation of ACAP4 is essential for CCL18-induced breast cancer cell migration and invasion, as overexpression of the persistent acetylation-mimicking or non-acetylatable ACAP4 mutant blocked CCL18-elicited cell migration and invasion. Mechanistically, the acetylation of ACAP4 at Lys311 reduced the lipid-binding activity of ACAP4 to ensure a robust and dynamic cycling of ARF6–ACAP4 complex with plasma membrane in response to CCL18 stimulation. Thus, these results present a previously undefined mechanism by which CCL18-elicited acetylation of the PH domain controls dynamic interaction between ACAP4 and plasma membrane during breast cancer cell migration and invasion.

Keywords: cell migration, acetylation, ACAP4, CCL18, PCAF, ARF6

Introduction

The tumor microenvironment comprises a variety of non-malignant stromal cells that play a pivotal role in tumor progression and metastasis (Raman et al., 2011). CCL18 belongs to the CC subgroup chemokines that regulates tumor cell growth, invasion, and metastasis (Kodelja et al., 1998; Condeelis and Pollard, 2006; Chen et al., 2011; Sakamoto, et al., 2016). Our recent study showed that chemokine CCL18 secreted from tumor-associated macrophage promotes cancer invasion and metastasis (Chen et al., 2011). However, the signaling pathways and mechanism underlying CCL18-elicited cellular dynamics in breast cancer cell migration and invasion remain less characterized (Bonecchi et al., 2011).

Cell migration plays a core role in a wide variety of biological phenomena, such as embryonic development, wound healing, immune response, and cancer metastasis (Jaffe and Hall, 2005; Kim et al., 2015; Ouellette et al., 2016). During cell migration, the coordination of membrane trafficking, actin skeleton remodeling, and formation of new adhesion complexes are required for protrusive activities at the leading edges of the migrating cells (D'Souza-Schorey and Chavrier, 2006; Gillingham and Munro, 2007; Shen et al., 2008; Du et al., 2010; Tilston-Lünel, et al., 2016). Some

Received April 13, 2018. Revised August 3, 2018. Accepted August 20, 2018.

small GTPases, such as ARF6, are important regulators of membrane trafficking and actin-based cytoskeleton dynamics at the leading edge of migrating cells (D'Souza-Schorey et al., 1995; Peters et al., 1995; Schafer et al., 2000; Donaldson and Jackson, 2011). Our previous study shows that ACAP4 is an ARF6 GTPase-activating protein that regulates membrane cytoskeletal dynamics in response to changes in extracellular cues (Fang et al., 2006; Ha et al., 2008; Ismail et al., 2010). The GAP activity of ACAP4 is regulated by phosphatidylinositol 4,5-biphosphate [PI(4,5)P_2] via binding to pleckstrin-homology (PH) domain (Fang et al., 2006). Beyond regulating EGF-stimulated membrane and cytoskeleton remodeling and actin-containing stress fiber formation, ACAP4 is also crucial in the process of EGF-elicited cell migration and invasion (Fang et al., 2006; Ha et al., 2008). Our recent study demonstrated that Tyr34 in the BAR domain of ACAP4 is phosphorylated in response to EGF stimulation. Phosphorylation of Tyr34 promotes the migratory activity of MDA-MB-231 cells (Zhao et al., 2013). Moreover, EGF stimulation induces phosphorylation of Tyr733, which enhances ACAP4 binding with Grb2. The ACAP4–Grb2 interaction not only regulates the trafficking of integrin 1 but also orchestrates the subsequent cellular dynamics such as cell adhesion, spreading, and migration (Yu et al., 2011). Dynamic changes in the plasma membrane and cytoskeleton during cell migration are orchestrated by spatiotemporal interactions among ARF6 GTPase, its guanine nucleotide exchange factors, and GTPase-activating proteins, which depend on regulated associations with phosphoinositides and ARF6 activity (Malaby et al., 2013). Several proteins containing the PH domain regulate actin-based cytoskeleton dynamics and cell migration (Macia et al., 2008; Donaldson and Jackson, 2011). In general, PH domain provides a spatiotemporal regulation of ARF6 interaction with its GAP proteins. However, the mechanism underlying the membrane association of these proteins via PH domain has remained undefined.

The present report demonstrates that the PH domain is essential for the recruitment of ACAP4 to the membrane structure and for its GAP activity. Importantly, Lys311 in the PH domain is acetylated in response to CCL18 stimulation. Acetylation of Lys311 in the PH domain modulates the membrane-binding activity and dynamics of ACAP4. This study revealed a previously undefined role for ACAP4 in linking ARF6-mediated membrane dynamics to chemokine CCL18-elicited cell migration and invasion.

Results

ACAP4 is essential for CCL18-elicited cell migration

Our early study revealed that chemokine CCL18 elicits breast cancer cell invasion and metastasis (Chen et al., 2011). Although a positive feedback loop between mesenchymal-like cancer cells and macrophages is postulated to regulate the cancer cell plasticity and subsequent metastasis (Su et al., 2014), however, the molecular mechanism underlying acute cellular response to CCL18 stimulation remains elusive. Given the function of ACAP4 in EGF-stimulated membrane dynamics and breast cancer MDA-MB-231 cell migration (Fang et al., 2006; Yu et al., 2011), we asked whether ACAP4 functions in CCL18-elicited cellular dynamics. To this end, we first examined the distribution of ACAP4 in MDA-MB-231 cells in response to CCL18 stimulation. As shown in Figure 1A, MDA-MB-231 cells were serum-deprived for 6 h followed by stimulation (20 ng/ml CCL18 for 10 min) or control vehicle. Examination of subcellular localization of ACAP4 relative to ARF6 revealed that both ACAP4 and ARF6 were primarily cytosolic with some concentration in endosome-like structure in serum-starved MDA-MB-231 cells (top panel, *a* and *b*), reminiscent what was seen in HeLa cells (Fang et al., 2006). Careful examination revealed that a fraction of ACAP4 was distributed to membrane ruffles where ARF6 was absent (top panel, *b*; arrows). Significantly, CCL18 stimulation triggered dramatic redistribution of ARF6 from the cytoplasm to the ruffles on the plasma membrane (bottom panel, *a'*; arrows). However, the localization of ACAP4 with membrane ruffles was diminished (bottom panel, *b'*). Quantitative analyses show that the ARF6-rich protrusion is a function of CCL18 stimulation in MDA-MB-231 cells (Figure 1B; $P < 0.01$).

To confirm whether the cellular response to CCL18 is cell line oriented, we carried out similar characterization using another triple negative breast cancer MDA-MB-468 cells. As shown in Supplementary Figure S1B, both ACAP4 and ARF6 were primarily cytosolic with some concentration in endosome-like structure in serum-starved MDA-MB-468 cells (top panel, *a* and *b*), reminiscent what was seen in MDA-MB-231 cell (Figure 1A). Consistent with what was seen in MDA-MB-231 cells, CCL18 stimulation triggered dramatic redistribution of ARF6 from the cytoplasm to the ruffles on the plasma membrane (bottom panel, *a'*; arrow). Quantitative analyses showed that the ARF6-rich protrusion is a function of CCL18 stimulation in MDA-MB-468 cells (Supplementary Figure S1C; $P < 0.01$). Thus, CCL18 stimulation triggers dynamic redistribution of ARF6 and ACAP4 in breast cancer cells.

To examine the function of endogenous ACAP4 underlying CCL18-elicited cell migration, MDA-MB-231 cells were depleted of ACAP4 by transfection with siRNA duplexes. Western blotting revealed that ACAP4 was efficiently depleted by specific siRNAs but not by scrambled sequences, whereas the levels of ezrin and ARF6 were unaffected (Figure 1C). We next tested whether ACAP4-depletion affects the cell migration using a wound-healing assay as previously described (Fang et al., 2006). Our western blotting analyses showed that two independent siRNAs (siRNA-1 and siRNA-2) efficiently suppressed the ACAP4 protein level in both MDA-MB-231 cells (Figure 1C) and MDA-MB-468 cells (Supplementary Figure S1D). As shown in Figure 1D, the wound in MDA-MB-231 cells became apparently healed at 8 h after CCL18 stimulation. However, the wound remained unhealed in the ACAP4-depleted cells (bottom panel). We scored cells that had migrated to wound area in response to CCL18 stimulation as presented in Figure 1E. In fact, the level of inhibition of migration observed in ACAP4-depleted cells was consistent and significant ($P < 0.01$) compared to the control siRNA-treated cells. In addition, the ACAP4 depletion-elicited inhibition of wound-healing phenotype was rescued when exogenous GFP-ACAP4 was expressed in MDA-MB-231 cells (Figure 1E) and MDA-MB-468 cells (Supplementary Figure S1E; $P < 0.01$). Therefore, these data suggest that endogenous ACAP4 is an important regulator responsible for the CCL18-elicited cell migration.

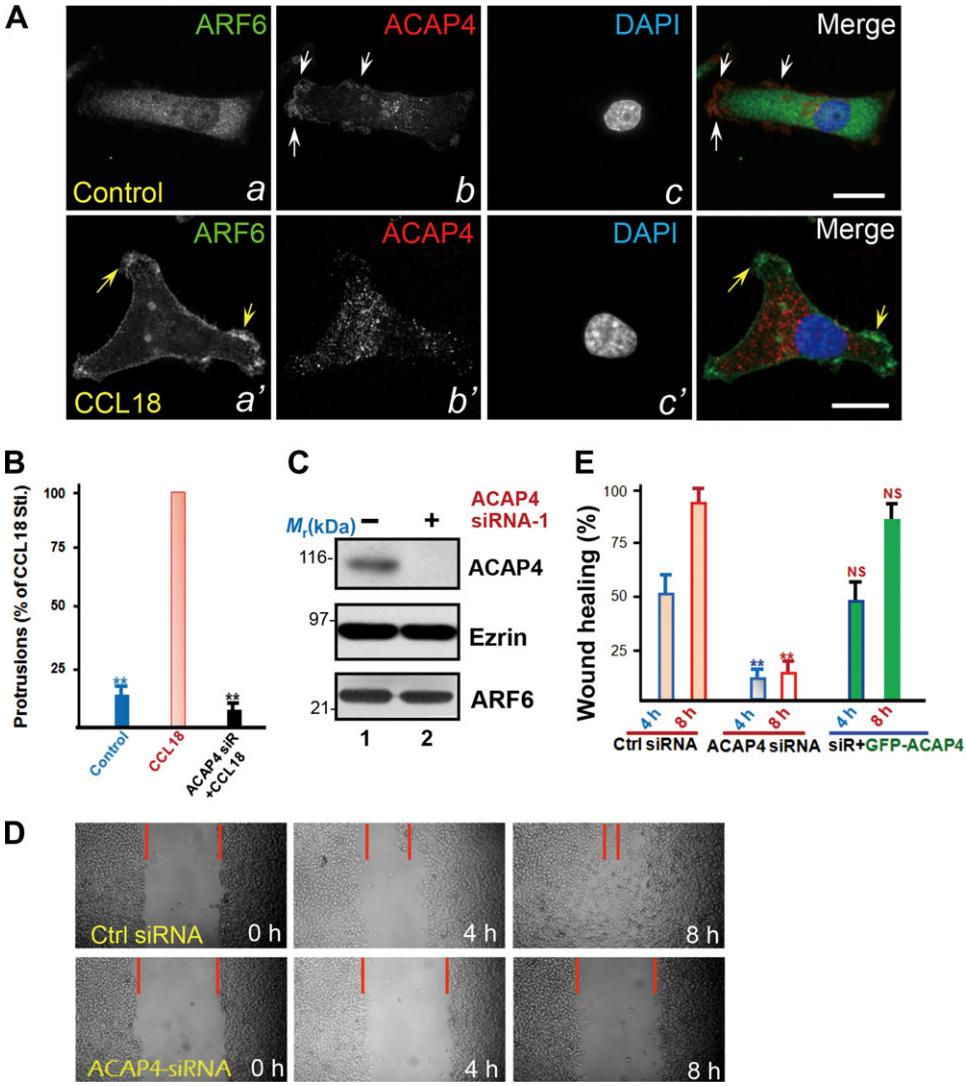

Figure 1 ACAP4 is required for CCL18-elicited breast cancer cell migration. (**A**) ARF6 and ACAP4 distribution profiles in the MDA-MB-231 cells. Breast cancer cells were starved from serum for 6 h before stimulated with 20 ng/ml CCL18 for 10 min. Cells were fixed, permeabilized, and stained for endogenous ARF6 (green), ACAP4 (red), and DAPI (blue). The merged montage was generated from three channels. Scale bar, 10 μm. (**B**) Quantitative analyses for the effect of ACAP4 on ARF6-dependent formation of protrusions. MDA-MB-231 cells were treated with scramble or ACAP4 siRNA for 24 h followed by CCL18 stimulation (20 ng/ml) for 10 min prior to fixation. The data are presented as the fraction of cells forming ARF6-rich protrusions normalized to the fraction of scramble siRNA-treated cells stimulated with CCL18. The error bars represent SEM; $n = 3$ preparations. (**C**) MDA-MB-231 cells were transfected with the ACAP4 siRNA oligonucleotides for 24 h and subjected to SDS-PAGE and immunoblotting. Top panel, immunoblot for ACAP4; middle panel, immunoblot for ezrin; bottom panel, immunoblot for ARF6. Scrambled oligonucleotides were used as controls. (**D**) Depletion of ACAP4 inhibits wound-healing cell migration. MDA-MB-231 cells treated with siRNA against ACAP4 or a scrambled control were examined in the wound-healing assay. Images were collected before or 4 and 8 h after the CCL18 addition (20 ng/ml). Results are representative of three independent experiments. (**E**) Quantitative analyses of wound-healing cell migration in **D**. The number of migrating cells depleted of ACAP4 to the wound area was compared with that of scrambled siRNA-treated MDA-MB-231 cells and then expressed as a percentage. The mean with SEM was then derived from three independent experiments. NS, no significant difference; $^{**}P < 0.01$.

Acetylation of ACAP4 at Lys311 is elicited by CCL18 stimulation

To elucidate the molecular mechanism underlying the function of ACAP4 in CCL18-elicited cell migration, we immunoisolated ACAP4 from CCL18-stimulated MDA-MB-231 cells (Figure 2A), which was confirmed by western blotting analyses (Figure 2B). Our proteomic analyses identified that ACAP4 Lys311 is acetylated in CCL18-treated but not control MDA-MB-231 cells (Figure 2C). Computational analyses indicated that CCL18-elicited lysine acetylation occurs in the PH domain of ACAP4 (Figure 2D).

To confirm that ACAP4 acetylation is elicited by CCL18 stimulation, MDA-MB-231 cells were treated with 20 ng/ml CCL18

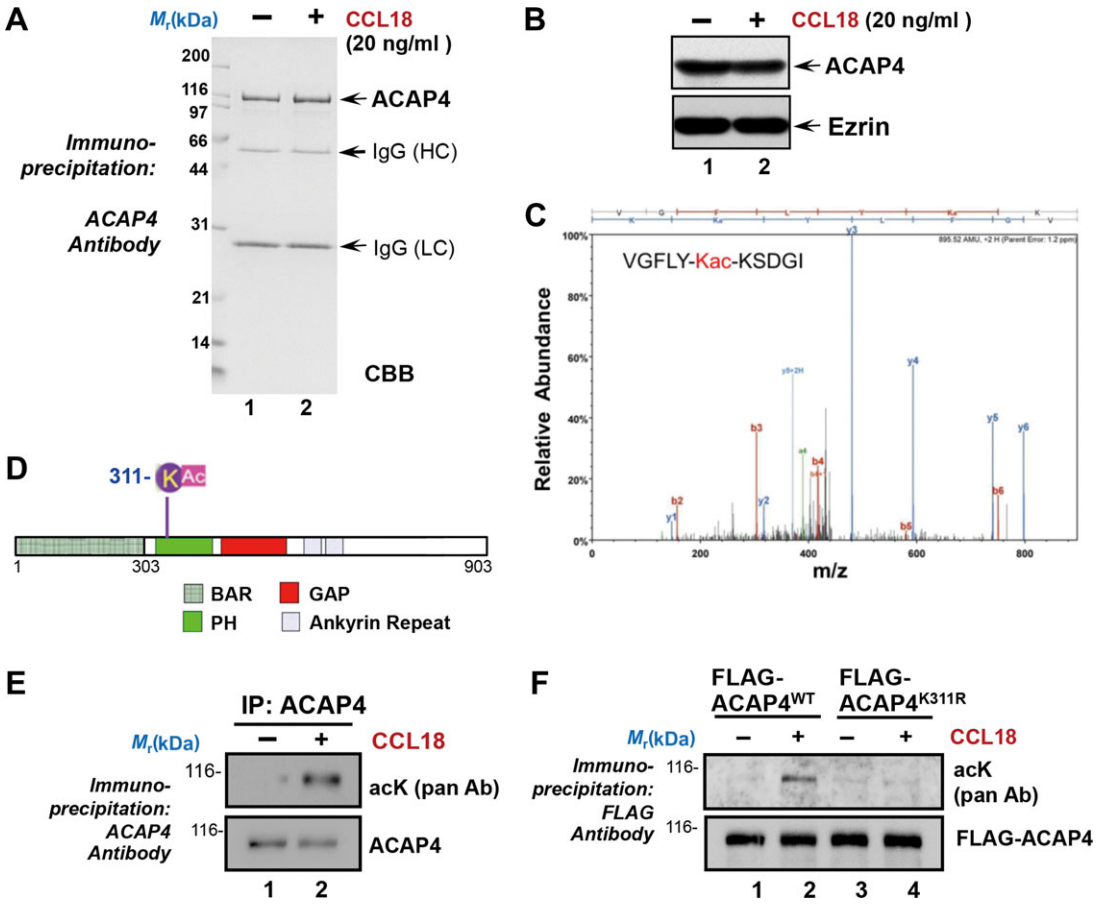

Figure 2 CCL18 stimulation elicits acetylation of ACAP4 at Lys311. (**A**) MDA-MB-231 cells were stimulated by CCL18 (20 ng/ml) followed by immunoprecipitation using anti-ACAP4 antibody-conjugated beads. After binding, anti-ACAP4 affinity matrix was extensively washed, and bound proteins were eluted with SDS sample buffer and separated by SDS-PAGE. (**B**) Western blotting analyses confirm the ACAP4 immunoprecipitation and the co-immunoisolation of ezrin. (**C**) Representative mass spectrum of acetylated Lys311 detected in CCL18-treated MDA-MB-231 cells. (**D**) Schematic diagram of ACAP4 structural features. Based on the amino acid sequence comparison, ACAP4 contains the BAR domain, PH domain, ARF GAP domain, and ANK repeat domains. Lys311 locates at the PH domain of ACAP4. (**E**) ACAP4 is acetylated in response to CCL18 stimulation. MDA-MB-231 cells were treated with 20 ng/ml CCL18 for 10 min followed by ACAP4 immunoprecipitation and subsequent immunoblotting with a pan-acetylated lysine antibody. Note that the ACAP4 band was reacted by pan-acetylated lysine antibody (acK pan Ab). (**F**) MDA-MB-231 cells were transiently transfected to express FLAG-ACAP4 wild-type and non-acetylatable mutant K311R. The transfected cells were treated with CCL18 as described above before anti-FLAG immunoprecipitation and anti-acetylated lysine blot. Note that the ACAP4 band was recognized by pan-acetylated lysine antibody (acK pan Ab).

(10 min) and subjected to an anti-ACAP4 antibody immunoprecipitation. The western blotting analyses of the ACAP4 immunoprecipitates with an anti-Lys acetylation antibody confirmed that endogenous ACAP4 protein was acetylated in response to CCL18 stimulation (Figure 2E). To further ascertain that Lys311 is acetylated in response to CCL18 stimulation, we constructed the ACAP4^{K311R} mutant by substituting the lysine residue with arginine (R). The MDA-MB-231 cells transfected with FLAG-ACAP4^{WT} and FLAG-ACAP4^{K311R} were treated with CCL18 as described above. The cells were subjected to immunoprecipitation with FLAG M2 beads. As shown in Figure 2F, acetylation level of FLAG-ACAP4^{K311R} was much lower than that of FLAG-ACAP4^{WT} (lane 4 vs. lane 2), indicating that acetylation of Lys311 of ACAP4 is a function of CCL18 stimulation in MDA-MB-231 cells.

ACAP4 is a cognate substrate of the acetyltransferase PCAF

Lysine acetylation is an important post-translational modification that regulates breast cancer recurrence and metastasis (Rios Garcia et al., 2017). However, no evidence shows the relationship between acetylation and ACAP4 in breast cancer cell invasion. The identification of acK311 in CCL18 stimulation prompted us to identify the upstream acetyltransferase responsible for ACAP4 acetylation. To this end, we performed immunoprecipitation assays, in which MDA-MB-231 cells were cotransfected with FLAG-ACAP4 and GFP-PCAF or GFP-TIP60. The transfected cells were then treated with CCL18 for 10 min in the presence of TIP60 inhibitor MG149 or PCAF inhibitor C146 (Bowers et al., 2010; Ghizzoni et al., 2012). The treated cells were then lysed and incubated with the anti-FLAG beads to isolate ACAP4 and its accessory proteins followed

by western blotting analyses. As shown in Figure 3A, the immunoblotting results with anti-acK311 antibody (acK311-ACAP4) confirmed that CCL18 stimulated ACAP4 acetylation at K311 (lane 2). Our pilot experiment indicated that PCAF but not TIP60 was associated with ACAP4. Indeed, our western blotting analyses confirmed that GFP-PCAF but not GFP-TIP60 was recovered in FLAG-ACAP4 immuoprecipitates (Figure 3A, third and bottom panels). In addition, the inhibition of PCAF by compound C146, but not TIP60, abolished acetylation of K311 on ACAP4 (lane 3), suggesting that ACAP4 interacts and is acetylated by the acetyltransferase PCAF in cells.

If ACAP4 acetylation is a function of PCAF, the two proteins may form a complex in MDA-MB-231 cells. To test this hypothesis, MDA-MB-231 cells were transiently cotransfected to express FLAG-PCAF with GFP-ACAP4 or GFP. As shown in Figure 3B, anti-FLAG antibody immunoprecipitated PCAF together with GFP-ACAP4 (lane 4) but not GFP (lane 3), revealing that PCAF formed a complex with ACAP4 in MDA-MB-231 cells. To confirm that the ACAP4–PCAF interaction is not cell line-oriented, we carried out an immunoprecipitation of endogenous ACAP4 and its associated proteins from MDA-MB-468 cells. As shown in Supplementary Figure S2, PCAF but not TIP60 was precipitated by an ACAP4 antibody (lane 2). In addition, ezrin, a component of ACAP4 complex, was also recovered in the precipitates (second panel, lane 2). Thus, PCAF is a cognate binding protein of ACAP4 in breast cancer cells.

Next, we sought to determine whether PCAF directly acetylates ACAP4 at Lys311. To this end, purified His-ACAP4^{WT} or His-ACAP4^{K311R} was incubated with GST-PCAF-TC in the absence or presence of Ac-CoA as previously described (Xia et al., 2012). Western blotting using anti-acK311 antibody confirmed that ACAP4 is a direct substrate of PCAF as PCAF acetylates wild-type ACAP4 but not ACAP4^{K311R} mutant (Figure 3C, lane 3). To further confirm whether ACAP4 is a substrate of PCAF in response to

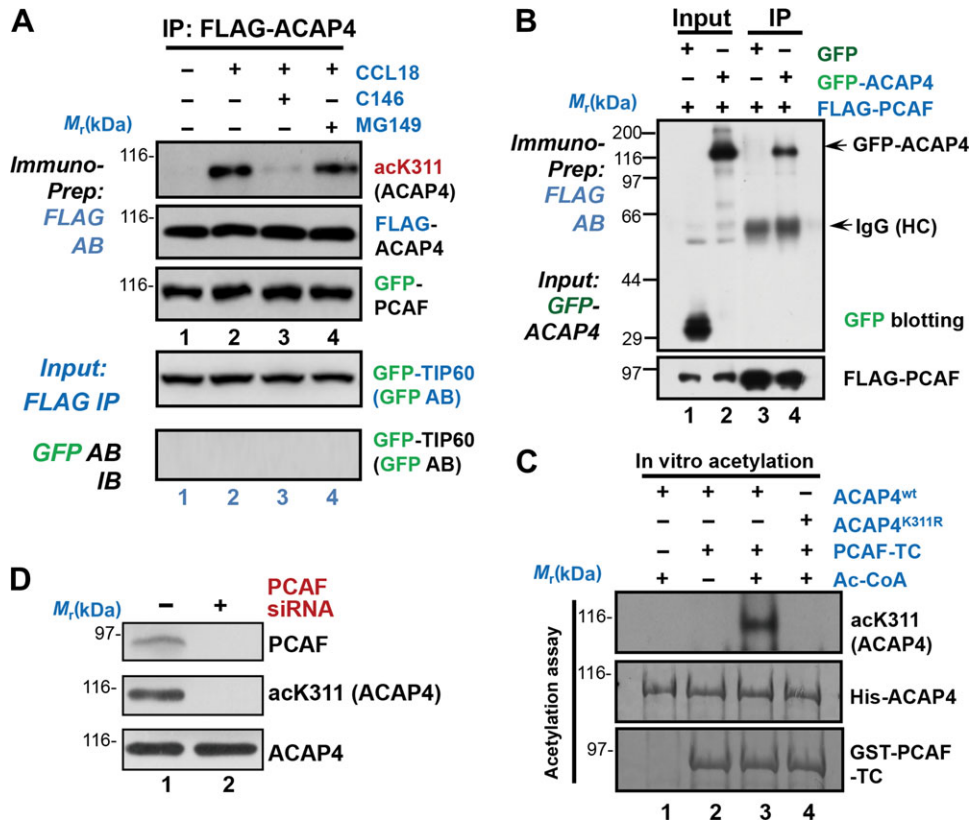

Figure 3 ACAP4 is a *bona fide* substrate of the acetyltransferase PCAF. (**A**) ACAP4 is acetylated by PCAF *in vivo*. MDA-MB-231 cells expressing FLAG-ACAP4 were pretreated with PCAF inhibitor C146 or TIP60 inhibitor MG149 for 30 min before exposure to CCL18 (20 ng/ml for 10 min). The FLAG-ACAP4 proteins were isolated by immunoprecipitation followed by western blotting with anti-acK311 antibody, anti-FLAG antibody, and anti-GFP antibody. (**B**) ACAP4 interacts with PCAF *in vivo*. MDA-MB-231 cells were transfected with GFP-ACAP4 and FLAG-PCAF. Twenty-four hours after transfection, cell lysates were incubated with the FLAG M2 beads for 4 h followed by western blotting with anti-GFP and anti-FLAG antibodies. (**C**) Lys311 of ACAP4 is acetylated by PCAF *in vitro*. His-ACAP4^{WT} and His-ACAP4^{K311R} proteins were incubated with GST-PCAF-TC and Ac-CoA at 30°C for 1 h. ACAP4^{WT} was acetylated in the presence of PCAF and Ac-CoA seen from anti-acK311 blot. However, no acetylation was detected in His-ACAP4^{K311R}. (**D**) Acetylation of ACAP4 at Lys311 is the function of PCAF. MDA-MB-231 cells were transfected to introduce PCAF siRNA and its control. Twenty-four hours after transfection, cell lysates were analyzed by western blotting using PCAF antibody to validate the knockdown efficiency and anti-K311ac-ACAP4 antibody to report the suppression of ACAP4 acetylation. Note that the PCAF depletion abolished the level of ACAP4 acetylation at Lys311, but not the level of ACAP4 protein.

CCL18 stimulation, MDA-MB-231 cells were transfected with PCAF siRNA and analyzed by western blotting with anti-acK311 antibody. As shown in Figure 3D, suppression of PCAF abolished CCL18-elicited acetylation of ACAP4 at Lys311. Therefore, we conclude that ACAP4 is a cognate substrate of PCAF in response to CCL18 stimulation.

CCL18-elicited acetylation promotes ARF6 activity by spatial regulation of ACAP4–ARF6 interaction

ACAP4–ARF6 interaction orchestrates membrane–cytoskeleton interaction during cell migration and invasion (Fang et al., 2006; Ha et al., 2008; Ismail et al., 2010). We therefore examined whether acetylation of ACAP4 regulates the interaction between ACAP4 and ARF6. To this end, 293T cells were transfected with Myc-ARF6 and FLAG-ACAP4 wild-type (WT) or its mutants (K311Q/R). The transfected cells were then lysed and subjected to anti-FLAG immunoprecipitation followed by western blotting analyses. As shown in Figure 4A and quantified in Supplementary Figure S3A, wild-type and acetylation-mimicking ACAP4 mutants did not exhibit any significant difference in ARF6 binding, suggesting that acetylation does not directly modulate ARF6 GTPase activity.

We next tested whether the acetylation of ACAP4 modulates ARF6 GTPase activity in MDA-MB-231 cells given the redistribution of ARF6 in response to CCL18 stimulation. Aliquots of MDA-MB-231 cells were transiently transfected to introduce ACAP4 siRNA and siRNA-resistant GFP-ACAP4 constructs (wild-type and acetylation-mimicking mutants). As shown in Supplementary Figure S3B, various GFP-ACAP4 constructs expressed at similar levels, while endogenous ACAP4 was suppressed (bottom panel). Next, we examined the levels of ARF6 GTPase in MDA-MB-231 cells expressing acetylation-mimicking mutants using a mono-specific antibody reacting ARF6-GTP. As shown in the top panel, the level of ARF6 GTPase is a function of CCL18 stimulation (lane 2). Consistent with previous reports (Fang et al., 2006; Ha et al., 2008), GAP-deficient mutant R469G protected ARF6-GTP from ACAP4-elicited hydrolysis (lane 5). In addition, the expression of acetylation-mimicking K311Q retained a higher level of ARF6-GTP compared to that of non-acetylatable mutant K311R (lanes 3 and 4), while the ARF6 protein levels did not change in MDA-MB-231 cells expressing various ACAP4 wild-type and mutant constructs. Quantitative analyses of the level of ARF6-GTP over ARF6 protein from three separate experiments confirmed that CCL18 increased the level of ARF6-GTP by ~5 folds (Supplementary Figure S3C). MDA-MB-231 cells expressing K311Q and R469G mutants contained higher levels of ARF6-GTP. Thus, we conclude that the acetylation of ACAP4 provides a spatial separation and protection of ACAP4 from ARF6 GTPase activity.

Our previous study showed that ACAP4 is a special GAP for ARF6 with an essential role in regulating the membrane trafficking and cell migration depending on its GAP activity toward ARF6 (Fang et al., 2006). To determine the ARF6 GTPase activity in response to CCL18 stimulation, we employed a pull-down assay using $GGA3^{GAT}$ as an affinity matrix to capture active ARF6 (Santy and Casanova, 2001). Specifically, MDA-MB-231 cells were stimulated with 20 ng/ml CCL18 or 0.1 μg/ml EGF followed by the GST-$GGA3^{GAT}$ pull-down assay. Active forms of ARF6 were measured by western blotting with an anti-ARF6-GTP antibody. As shown in Figure 4B, the $GGA3^{GAT}$ pull-down assay showed that both CCL18 and EGF treatments increased ARF6 GTPase activity. Quantitative analyses from three independent experiments indicated that CCL18 or EGF stimulation increased ARF6 activity by 2.2 ± 0.4 folds and 3.9 ± 0.3 folds, respectively (Figure 4C).

Given the increased ARF6 GTPase activity seen in CCL18 stimulation and unchanged ARF6–ACAP4 interaction observed in pull-down assay, we reason that CCL18 may regulate ACAP4 and ARF6 in a spatial manner. To this end, MDA-MB-231 cells were transiently transfected to express GFP-ACAP4 wild-type and acetylation mutants followed by stimulation with CCL18. The stimulated MDA-MB-231 cells were then fixed and immunostained with ARF6. As shown in Figure 4D, CCL18 stimulation elicited a relocation of ARF6 to the membrane ruffles (*b*; arrows). However, wild-type and persistent acetylation-mimicking mutant GFP-$ACAP4^{K311Q}$ were largely seen as cytoplasmic (*d* and *f*). Interestingly, non-acetylatable mutant GFP-$ACAP4^{K311R}$ was apparently seen at membrane ruffles (*h*; arrows). Quantitative analyses showed variation of ACAP4-rich protrusion upon Lys311 acetylation in MDA-MB-231 cells (Figure 4E; $P < 0.01$). Thus, acetylation of K311 may serve as a dynamic tune for ACAP4 association with membrane.

To evaluate whether acetylation of K311 tunes ACAP4 membrane binding to cytosol, we sought to assess the partitioning of ACAP4 in membrane and cytosolic fractions using digitonin extraction protocol as previously described (Ding et al., 2008). Specifically, MDA-MB-231 cells were transfected with GFP-$ACAP4^{WT}$ or acetylation mutants GFP-$ACAP4^{K311Q}$ and GFP-$ACAP4^{K311R}$. Twenty-four hours after transfection, the cells were stimulated with CCL18 followed by digitonin extraction of MDA-MB-231 cells. As shown in Figure 4F, ACAP4 was present largely in the plasma membrane of non-stimulated cells (lane 1). CCL18 stimulation induced the translocation of GFP-$ACAP4^{WT}$ and GFP-$ACAP4^{K311Q}$, from the plasma membrane to cytosol (lanes 4 and 8). This CCL18-induced translocation exhibited little impact on GFP-$ACAP4^{K311R}$ (lanes 5 and 6), suggesting that acetylation of ACAP4 tunes ACAP4 from membrane-binding to cytosolic localization. Quantitative analyses from three independent preparations validated that acetylation of Lys311 liberated ACAP4 from the digitonin-insoluble membrane fraction to cytosol fraction (Figure 4G). Thus, we conclude that acetylation of Lys311 serves as a dynamic switch for homeostatic association/dissociation of ACAP4 to plasma membrane.

To assess the dynamics of K311 acetylation and endogenous ACAP4 protein cellular re-localization following CCL18 treatment, we carried out western blotting analyses of K311 acetylation of endogenous ACAP4 and the relocation of ACAP4 protein in response to CCL18 stimulation using the digitonin protocol mentioned above. As shown in Supplementary Figure S4A, ACAP4 protein level increased in response to CCL18 stimulation (middle panel, lane 4), and this relocation was blocked by PCAF inhibitor

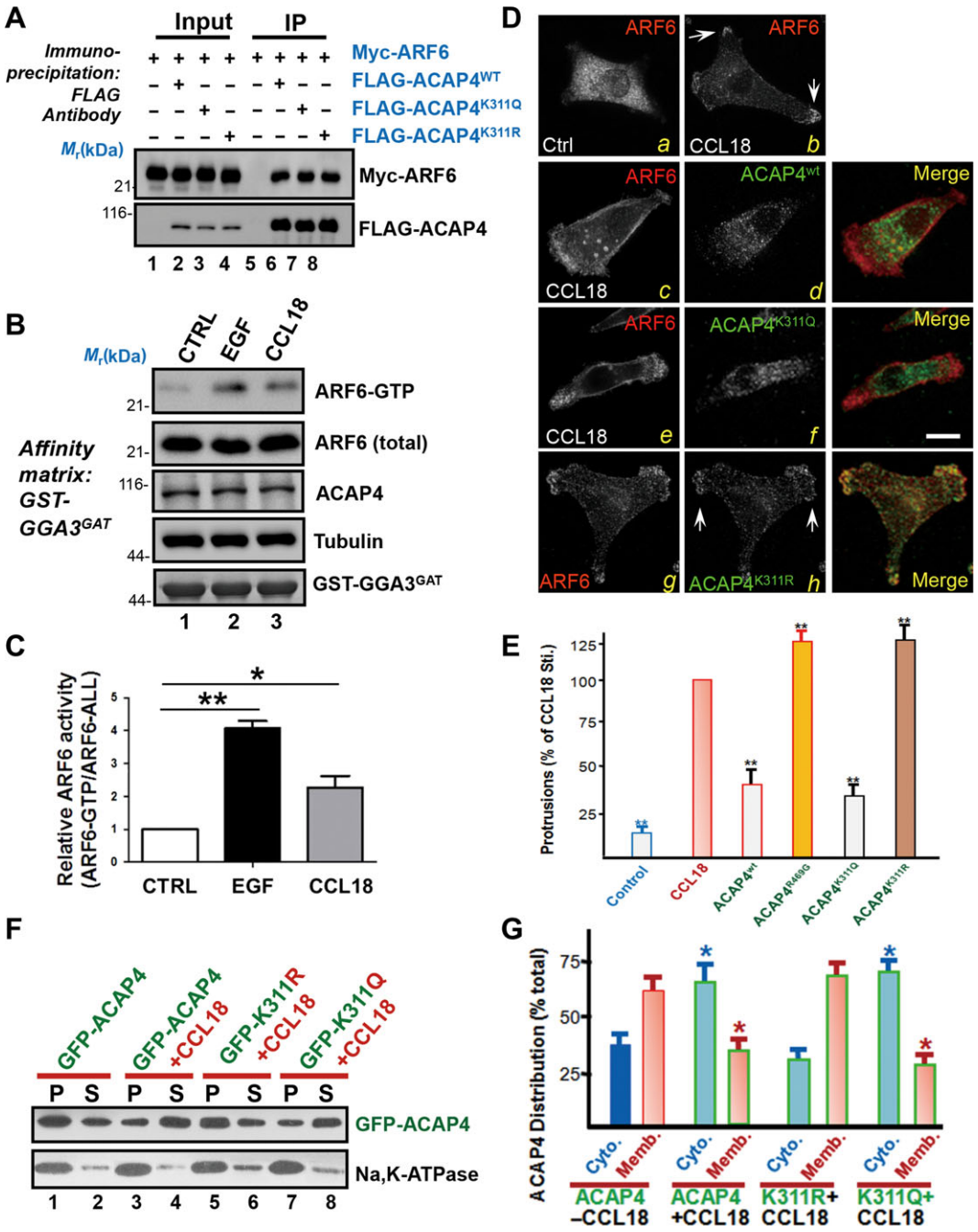

Figure 4 CCL18-elicited acetylation promotes ARF6 GTPase activity via dissociation of ACAP4 from the plasma membrane. (**A**) Co-immunoprecipitation of Myc-ARF6 and FLAG-ACAP4 wild-type or variants. 293T cells were transfected with Myc-ARF6 plus FLAG-ACAP4 wild-type (WT) or variants (K311Q/R). Twenty-four hours after transfection, cells were lysed and incubated with the FLAG M2 beads for 2 h. Then the beads were washed and analyzed by western blotting with anti-Myc and anti-FLAG antibodies. (**B**) Endogenous ARF6 activity was measured by GGA3 pull-down assay with CCL18 simulation. MDA-MB-231 cells were subjected to serum starvation followed by stimulation with 20 ng/ml CCL18 for 10 min or 0.1 μg/ml EGF for 5 min. The stimulated cells were incubated with the GST-GGA3^{GAT}. Active forms of ARF6 were measured by anti-ARF6-GTP blot. (**C**) Quantitative analyses on the ratio of ARF6-GTP/ARF6-ALL described in **B**. Data represent mean ± SEM from three independent experiments. *$P < 0.05$, **$P < 0.01$. (**D**) MDA-MB-231 cells were transfected with ACAP4-GFP wild-type (WT) or acetylation-mimicking variants (K311Q/R). At 16 h after transfection, cells were subjected to CCL18 stimulation. Treated cells were fixed and then examined under fluorescence microscope. Note that persistent acetylation mutant or CCL18 stimulation attenuated the membrane-associated ACAP4 localization. Scale bar, 10 μm. (**E**) Quantitative analyses of membrane protrusion rich in ARF6. Data represent mean ± SEM from three independent experiments. **$P < 0.01$. (**F**) CCL18 stimulation liberates ACAP4 from plasma membrane association. MDA-MB-231 cells were transfected with ACAP4-GFP wild-type (WT) or acetylation-mimicking variants (K311Q/R). At 16 h after transfection, cells were subjected to CCL18 stimulation followed by digitonin extraction to separate cytosol from membrane fraction. (**G**) Quantitative analyses of ACAP4 partitioning in membrane and cytosol. Data represent mean ± SEM from three independent experiments. *$P < 0.05$.

C146, indicating that CCL18-elicited ACAP4 relocation is mediated by PCAF. Consistent with what was seen in ACAP4 protein relocation, CCL18 treatment dramatically increases the level of acetylated ACAP4 (acK311) in the cytosol fraction (top panel, lane 4). The rise of acK311 in cytosol was blocked by pretreatment of PCAF inhibitor C146. Quantitative analyses indicated that CCL18 stimulation induced an ~5.3-fold increase of acK311 in the cytosol fraction, while C146 treatment completely blocked the redistribution of acetylated ACAP4 (Supplementary Figure S4B; $^{**}P < 0.01$, $^{*}P < 0.05$). Thus, CCL18 treatment induces a dynamic K311 acetylation and relocation of ACAP4 in a PCAF-dependent manner.

Acetylation at Lys311 modulates membrane-binding activity of ACAP4

In our previous study, the GAP activity of ACAP4 was regulated by $PI(4,5)P_2$ via PH domain (Schafer et al., 2000). Our computational analyses revealed that Lys311 resided a critical position in PH domain, which composes the $PI(4,5)P_2$-binding pocket (Jian et al., 2015). To understand whether the acetylation at Lys311 directly disrupts the membrane-binding capacity of ACAP4 *in vitro*, we compared the affinity to phospholipids between ACAP4 wild-type and mutants using Echelon PIP strip (Figure 5A). PIP strips spotted with 15 different biologically active lipids were incubated with recombinant His-$ACAP4^{WT}$, $ACAP4^{K311Q}$, and $ACAP4^{K311R}$ as previously described (Zhao et al., 2013). We observed that the acetylation-mimicking (K311Q) mutant bound with a specifically decreased affinity to $PI(4,5)P_2$, whereas all the recombinant proteins showed less difference in other tested phospholipids (Figure 5B). The deficiency in membrane binding ability of acetylation-mimicking mutant $ACAP4^{K311Q}$ was also observed in the liposome sedimentation assay (Figure 5C). Quantitative analysis on the liposome-binding fractions revealed a dramatic reduced liposome-binding capacity in the $ACAP4^{K311Q}$ fraction (Figure 5D). Our previous study using the electron microscopy figured that the BAR domain of ACAP4 could tubulate the membrane *in vitro*. To determine the role of Lys311 acetylation in the membrane binding and sculpture, we constructed truncated $ACAP4^{1–424}$ (only including N-terminal BAR and PH domain) and mutants. Liposomes were incubated with His-$ACAP4^{1–424/WT}$, $ACAP4^{1–424/K311Q}$, or $ACAP4^{1–424/K311R}$, respectively, followed by electron microscopic analyses. As shown in Figure 5E, $ACAP4^{1–424/WT}$ and $ACAP4^{1–424/K311R}$ significantly changed the shape of the LUV, but we did not observe any bending or tabulation on the LUV with $ACAP4^{1–424/K311Q}$. Taken together, we conclude that the acetylation at Lys311 of PH domain strongly attenuates the membrane-binding ability of ACAP4.

Acetylation of K311 orchestrates CCL18-elicited cell motility

We next sought to examine the function of acK311 in regulating ACAP4 activity in CCL18-elicited cell migration. MDA-MB-231 cells were transiently transfected to introduce siRNA targeted to the 3′-UTR of ACAP4 and GFP-ACAP4 constructs. As shown in Figure 6A, western blotting with an anti-ACAP4 antibody revealed that the siRNA caused remarkable suppression of ACAP4 protein level at 24 h, whereas control cells treated with scramble oligonucleotides expressed normal level of ACAP4. Exogenous GFP-ACAP4 (wild-type and mutant) constructs expressed comparable level of ACAP4 protein as that of endogenous ACAP4. To examine the role of acK311 in cell motility, we monitored MDA-MB-231 cell migration using a wound-healing assay as shown in Figure 1D. The confluent MDA-MB-231 cells expressing various GFP-ACAP4 in the absence of endogenous ACAP4 were scratched with a 20-μl pipet tip followed by scoring the cells that had migrated to wound area in response to CCL18 stimulation. As shown in Figure 6B, statistical analyses from three independent experiments showed that GFP-ACAP4 (siR+ACAP4) sustained CCL18-elicited cell migration similar to that of MDA-MB-231 cells without depletion of endogenous ACAP4 (control siRNA). Expression of persistent acetylation-mimicking mutant (siR+K311Q) resulted in greater suppression of cell migration ($P < 0.01$), while MDA-MB-231 cells expressing non-acetylatable mutant (siR+K311R) partially healed the wound, suggesting that dynamic acetylation of K311 ensures efficient cell migration.

To examine the role of acetylation of Lys311 in CCL18-elicited cell migration, we monitored the real-time trajectory of MDA-MB-231 cells expressing wild-type and acetylation-mimicking mutants as previously reported (Zhao et al., 2013). Our trial experiment showed that MDA-MB-231 cells exhibit locomotion in the absence of CCL18 and addition of CCL18 triggered directional movement of MDA-MB-231 cells (Supplementary Figure S5A). Interestingly, this directional migration required ACAP4, as suppression of ACAP4 abolished the directional movements of MDA-MB-231 cells.

We next examined the migration distance in the absence of ACAP4 as illustrated in Figure 6C. As summarized in Supplementary Figure S5B, suppression of ACAP4 cut down the total distance of travel from initial to final point upon stimulation with CCL18. Quantitative analyses showed that the distance traveled by the cells expressing K311Q and K311R was ~80% of that in control cells expressing wild-type ACAP4 (Supplementary Figure S5B, $P < 0.01$). Importantly, our quantitative analyses of directional distance revealed that the distance of directly cell migration in the cells expressing K311Q and K311R was only 25%–33% of that in control cells expressing wild-type ACAP4 (Figure 6D). In addition, suppression of ACAP4 abolished the CCL18-elicited directional cell migration. Thus, we conclude that ACAP4 is required for directionally persistent cell migration in MDA-MB-231 cells.

We next examined the role of acetylation at Lys311 in CCL18-elicited cell invasion using a Boyden chamber assay. Specifically, MDA-MB-231 cells expressing various GFP-ACAP4 in the absence of endogenous ACAP4 were added to the Boyden chamber 24 h after transfection and stimulated with 20 ng/ml CCL18 or PBS as control. Four hours after the stimulation, migrated cells were imaged and counted. As shown in Figure 6E, depletion of ACAP4 or PCAF significantly suppressed the invasion. MDA-MB-231 cells expressing $ACAP4^{K311Q}$ mutant failed, while a few of MDA-MB-231 cells expressing non-acetylatable $ACAP4^{K311R}$ mutant passed

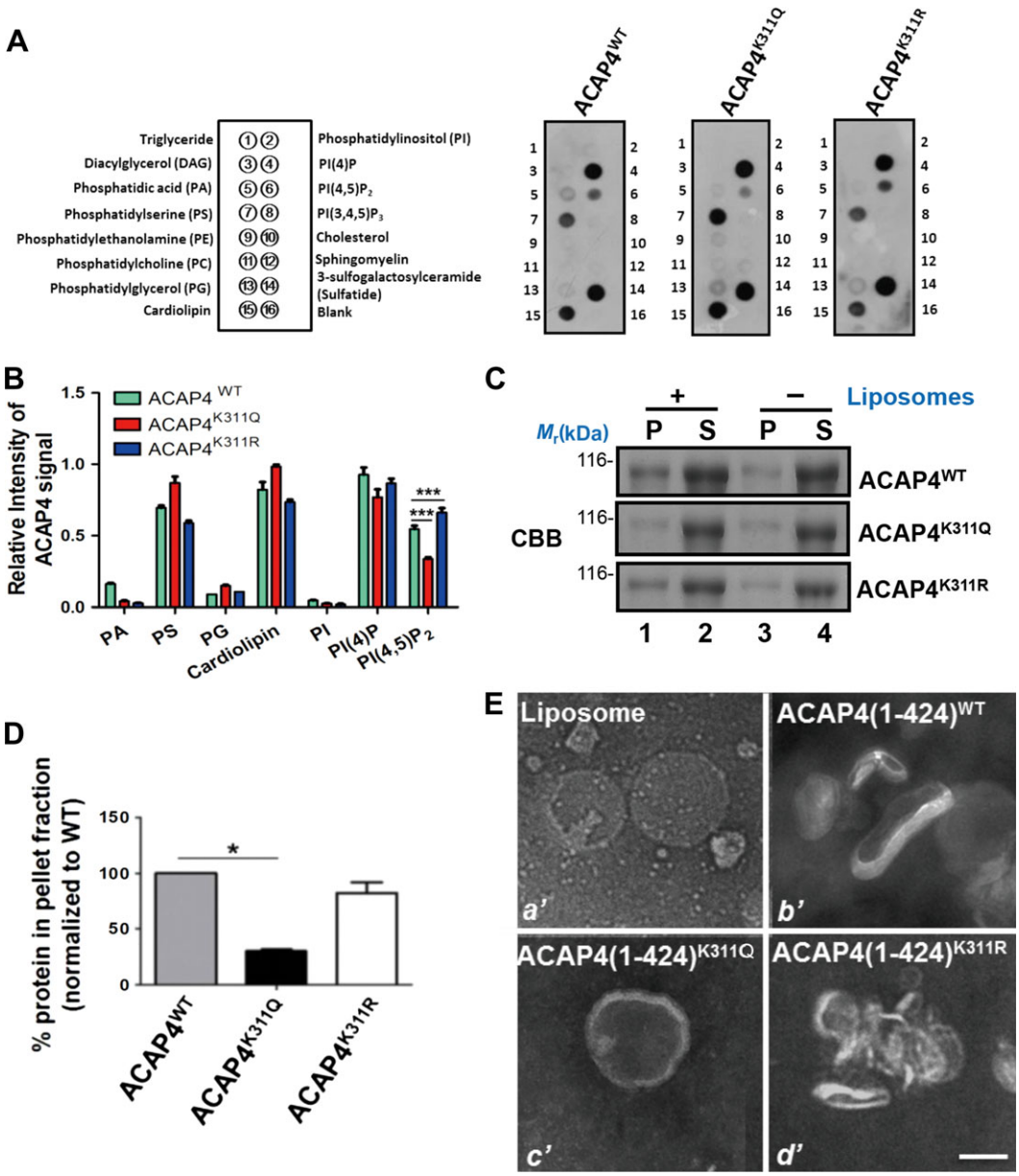

Figure 5 Acetylation at Lys311 modulates membrane association of ACAP4. (**A**) Characterization of ACAP4 binding to phospholipids. Three sets of Echelon PIP strips spotted with 15 different biologically active lipids (left panel) were incubated with recombinant His-ACAP4^{WT}, His-ACAP4^{K311Q}, or His-ACAP4^{K311R}, respectively. (**B**) Quantitative analyses of phospholipids binding activity. Relative intensity of each binding spot was normalized by the most intensive spot. Note that acetylation of ACAP4 at Lys311 attenuated the ACAP4-PI(4,5)P_2 interaction. Data represent mean ± SEM; ***$P < 0.001$; $n = 3$. (**C**) His-ACAP4^{WT}, His-ACAP4^{K311Q}, and His-ACAP4^{K311R} proteins were incubated with LUVs. The pellet (P) and supernatant (S) components were fractionated by centrifugation, and then analyzed by SDS-PAGE. (**D**) Quantitative analyses of liposome-binding activity. Data represent mean ± SEM; *$P < 0.05$; $n = 3$. (**E**) Electron micrographs of LUVs made from total brain lipids and incubated with the His-ACAP4 $^{1–424/WT}$, His-ACAP4$^{1–424/K311Q}$, and His-ACAP4$^{1–424/K311R}$ proteins. The WT and K311R mutant but not K311Q mutant of ACAP4 induce tubular structures. Scale bar, 100 nm.

through the Boyden chamber. Quantitative analyses indicated that CCL18-elicited breast cancer cell invasion depended on activity of ACAP4, PCAF, and PITPNM3 (Figure 6F). These results indicate that dynamic acetylation of Lys311 facilitates CCL18-elicited cell migration and invasion.

Discussion

This study reveals ACAP4, which is a cognate substrate of PCAF, is acetylated in Lys311. This CCL18-elicited acetylation plays a critical role in the membrane–cytoskeleton dynamics and cell migration by regulating ARF6 activity. Interestingly, this

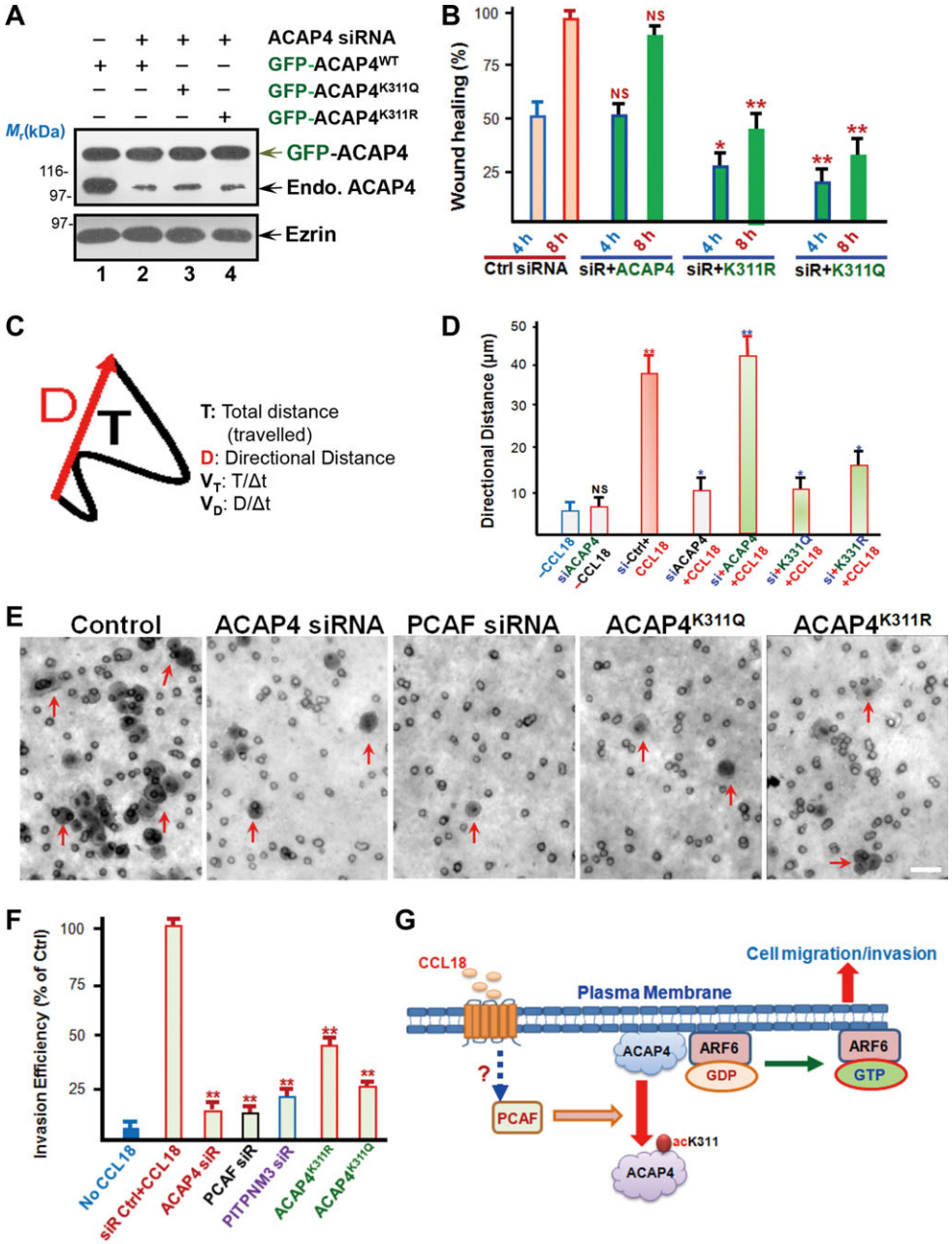

Figure 6 Acetylation of K311 orchestrates CCL18-elicited breast cancer cell migration and invasion. (**A**) Western blotting analyses of exogenous expression of GFP-ACAP4 wild-type and K311Q/R mutants in MDA-MB-231 cells. (**B**) Acetylation of Lys311 is necessary in MDA-MB-231 cell migration. MDA-MB-231 cells were transfected with WT or the K311Q/R mutants of ACAP4. Wound-healing assay was performed as in Figure 1D and the migrated cells were counted. Quantitative analyses of migration ratio are shown. Data represent mean ± SEM. NS, no significant difference; $*P < 0.05$; $**P < 0.01$; $n = 3$. (**C**) Schematic drawing of cell migration trajectory. The total distance between the starting and ending points (*T*) and the actual trajectory (*D*) are indicated. (**D**) Quantitative analyses of directional distance. Data represent mean ± SEM. $n = 31$ and 29, respectively. $*P < 0.05$; $**P < 0.01$. (**E**) PCAF–ACAP4 signaling is essential for MDA-MB-231 cell invasion. MDA-MB-231 cells were transfected with ACAP4 WT or K311Q/R mutants and set to the Boyden chamber assay. Invasive cells through the membrane were stained and imaged. Note that the cells passing through the Boyden chamber were indicated by arrows. (**F**) Quantitative analyses of invasion efficiency shown in **E**. Data represent mean ± SEM. $**P < 0.01$; $n = 3$. (**G**) Working model. In breast cancer cells, CCL18 binds to its receptor on the plasma membrane of breast cancer cells and transacts PCAF activity. PCAF-acetylated ACAP4 binds to the plasma membrane and induces the release of ACAP4 to the cytosol. Meanwhile, ARF6 is recruited to the plasma membrane by the CCL18 signal; the spatial separation of ACAP4 from ARF6 at the plasma membrane enhances the ARF6 GTPase activity. We propose that the dynamic cycling of ACAP4 between membrane and cytosol accounts for the drive behind ARF6- and ACAP4-dependent cell migration and invasion.

acetylation at Lys311 resides in the PH domain, which is critical to ACAP4 by virtue of its membrane targeting function and GAP activity modulation by the $PI(4,5)P_2$. Acetylation of Lys311 provides a link between CCL18 stimulation and membrane dynamics in directional cell migration and invasion. These results establish a previously uncharacterized regulatory mechanism governing ACAP4-associated membrane dynamics through acetylation-mediated regulation of the PH domain.

The function of the acetylation site in the PH domain has not been well understood because of the low degree of conservation in acetylation motifs. But it is worth noting that Lys311 is highly conserved in the subfamily of ARF GTPase-activating proteins such as ACAP1, ACAP2, ASAP1, and ASAP2 (Supplementary Figure S1A). This residue is critical to the PH domain in the interaction with $PI(4,5)P_2$ (Jian et al., 2015). Our early study showed that the ACAP4 GAP activity is modulated by $PI(4,5)P_2$ via PH domain (Fang et al., 2006). This finding provides a new mechanism of acetylation in regulating membrane binding capacity and the activity of ARF GTPases. The BAR domain of ACAP4 undergoes dimerization to produce a curved protein structure to sense and impart membrane curvature (Zhao et al., 2013). It has recently been demonstrated that the PH domain functions together with the adjacent BAR domain in regulating ACAP1 interaction with membrane (Pang et al., 2014). Thus, we reason that acetylation-elicited dissociation from $PI(4,5)P_2$ cooperates with the BAR domain to sense the curvature and components of the membrane in the intracellular environment, and plays an important regulation in ACAP4 activity in space for driving cellular dynamics. It would be a common structural feature and regulatory mechanism underlying PH-BAR domain-containing proteins, such as AZAP families, during context-regulated cellular dynamics. This mechanism, observed frequently in signaling pathways, gives rise to precise spatial regulation in localizing binding partners and enzymatic activities as illustrated in our working model (Figure 6G).

Cell migration is a highly orchestrated process that occurs during embryonic development, wound healing, immune response, cancer metastasis, and bacterial infections (Kolaczkowska and Kubes, 2013; Nieto, 2013; Ouellette et al., 2016; Tilston-Lünel et al., 2016). Our early study revealed that chemokine CCL18 promotes cancer cell invasiveness by triggering integrin cluster and enhancing the adherence to extracellular matrix by binding with its receptor, PITPNM3 (Chen et al., 2011). Zhang et al. (2013) further demonstrated that CCL18 signaling induces an epithelial-mesenchymal transition via Akt–GSK3–Snail pathway, thus promoting the invasion and metastasis of breast cancer. Our current study uncovered the molecular mechanisms underlying CCL18-elicited breast cancer cellular dynamics. The excitement and challenge ahead are to delineate how the PCAF–ACAP4–ARF6 signaling cascade synergizes with the Akt–GSK3β–Snail pathway in space and time during CCL18-elicited breast cancer cell migration and invasion using a spectral imaging approach recently established combined with context-specific organoids model system (Valm et al., 2017).

Lysine acetylation is an important post-translational modification that regulates gene transcription by targeting histones (Malaby et al., 2013). Non-histone protein acetylation in cancer cells regulates diverse biological functions that have been associated with precision cell division control, tumorigenesis, and cancer progression (Macia et al., 2008; Malaby et al., 2013; Rios Garcia et al., 2017). Our studies revealed that ACAP4 is involved in several signaling pathways such as EGF (Yu et al., 2011; Zhao et al., 2013) and CCL18–PCAF signaling pathway established in this report. Future work will be directed to delineate how CCL18 stimulation modulates PCAF activity and whether EGF cross-talks with CCL18 in breast cancer cell invasion and metastasis. Our current study suggests that ACAP4 is preferentially enriched within membrane microdomains with high curvature in the presence of components such as $PI(4,5)P_2$ using PH and BAR domains. It would be of great interest to annotate a nanoscale organization of the ACAP4 BAR and PH domains with different lipid partition profiles using pair correlation analysis combined with photo-activation localization microscopy (Sengupta et al., 2011; Xia et al., 2014a; Sakamoto et al., 2016), and to determine whether acetylation of Lys311 and/or phosphorylation of Tyr34 alters its spatial localization.

The present results demonstrate that acetylation at the Lys311 site in the PH domain of ACAP4 regulates the dynamic interaction of ACAP4 with the plasma membrane in response to chemokine CCL18 stimulation. During breast cancer cell migration and invasion, this dynamic membrane association/dissociation by the ACAP4 PH domain regulates ARF6 GTPase activity and dynamics in CCL18-stimulated membrane–cytoskeleton remodeling in a spatial order. Further, dynamic acetylation of Lys311 promotes the directional motility of MDA-MB-231 cells in cell migration and invasion. Thus, the results provide insights on the regulation of ARF6 activity by ACAP4 in the CCL18 signaling pathway during breast cancer cell invasion and perhaps metastasis.

Materials and methods

Plasmid construction

Site-directed mutants of FLAG-, GFP-, or His-tagged ACAP4 were generated by PCR-based, site-directed mutagenesis kit (C212) from Vazyme according to the manufacturer's instructions. Constructs of FLAG-, GFP-, GST-, and His-tagged proteins were generated by subcloning the indicated cDNAs into p3×FLAG-myc-CMV-24 (Sigma), pEGFP-N1 (Clontech), pGEX-6P-1 (GE Healthcare), and pET-22b (Novagen), respectively. mCherry-tagged ARF6 (mCherry-ARF6 fusion was cloned into pcDNA3.1-vector) and siRNA-resistant ACAP4 expression constructs were also constructed and used in this study as previously described (Xia et al., 2014b). To generate the GST-fusion proteins of PCAF-TC and $GGA3^{GAT}$, the sequence for the C-terminal PCAF (352–832), N-terminal GGA3 (1–303) was amplified by PCR and subcloned into pGEX-6P-1 vector. The N-terminal (1–424) of ACAP4 was subcloned into pET-22b vector to produce His-ACAP4 fusion proteins. All plasmid constructs were sequenced for verification.

Antibodies, inhibitors, and drugs

Anti-FLAG M2 antibody and anti-α-tubulin (DM1A) antibody were purchased from Sigma. Anti-GFP antibody was purchased from BD Biosciences. Anti-HA antibody, anti-Myc antibody, anti-ARF6 antibody and anti-acetylated-lysine antibody were purchased from Cell Signaling Technology. Anti-ARF6-GTP antibody was purchased from NewEast Biosciences. TSA (1 μM) and digitonin (0.1% *v/v*) were purchased from Sigma. C146 (2 μM) was purchased from Chembridge. MG149 (80 μM) was purchased from Axon. CCL18 (20 ng/ml) was purchased from Invitrogen. EGF (0.1 μg/ml) was purchased from Calbiochem. Anti-ACAP4 antibody was generated as described by Fang et al. (2006). To generate anti-acK311 ACAP4 antibody, peptide containing acetylated K311 (KVGFLY-acK-KSDGIRR) was conjugated to rabbit albumin (Sigma) and immunized into rabbits as previously described (Yao et al., 1997). The serum was collected and pre-absorbed by unacetylated ACAP4 peptide (KVGFLYKKSDGIRR) followed by affinity-purification using (KVGFLY-acK-KSDGIRR)-conjugated sulftone Sepharose beads (Sigma) (Yao et al., 1997). The specificity of the antibody has been extensively characterized using siRNA-mediated suppression of PCAF and ACAP4.

Cell culture and transfection

MDA-MB-231, MDA-MB-468, and 293T cells were obtained from the American Type Culture Collection (ATCC) and cultured in DMEM (Gibco) containing 10% FBS (Hyclone), 100 U/ml penicillin (Gibco), and 100 μg/ml streptomycin (Gibco). MDA-MB-231 and MDA-MB-468 cells were obtained from the ATCC and cultured in L-15 medium (Gibco) containing 10% (*v/v*) FBS. All cell lines were cultured at 37°C. Cells were transfected with plasmids using Lipofectamine 2000 (Invitrogen) according to the manufacturer's instructions.

siRNA treatment and measurement for knockdown efficiency

Double-stranded 19-nucleotide RNA duplex targeted to ACAP4 (siRNA-1, 5′-TCTCACACAGCACGATAAA-3′; siRNA-2, 5′-CAACAAGA CCTATGAGACT-3′) was purchased from Dharmacon Research Inc. as previously reported (Ding et al., 2010; Yu et al., 2011; Zhao et al., 2013). As a control, either a duplex targeting cyclophilin or scrambled sequence was used (Yuan et al., 2017). In brief, cultured parietal cells were transfected with siRNA oligonucleotides or control scrambled oligonucleotides, whereas the efficiency of this siRNA-mediated protein suppression was judged by western blotting analysis.

Recombinant protein expression

GST-PCAF-TC (352–832 amino acids), GST–GGA3^{GAT} (1–303 amino acids), as well as His-ACAP4 wild-type and mutants were expressed in BL21 (DE3) or Rosetta (DE3) at 30°C for 4–6 h and purified using Ni-NTA agarose (Qiagen) or glutathione Sepharose 4B resin (GE Healthcare) according to the manufacturer's instructions.

Immunoprecipitation

293T cells transfected with indicated plasmids were lysed in lysis buffer (20 mM Hepes, pH 7.4, 150 mM NaCl, 1mM EDTA, 0.1% Triton X-100) at 4°C. Lysates were clarified by centrifugation at 12000 rpm for 20 min at 4°C and then incubated with FLAG M2 beads (Sigma) at 4°C for 4 h. After washed with Hepes buffer for three times, the beads were boiled in SDS-PAGE sample buffer for 10 min. The bound proteins were separated by SDS-PAGE and immunoblotted with the indicated antibodies.

Immunofluorescence and microscopic analyses of cell migration

MDA-MB-231 cells transfected with indicated plasmids were fixed in 3.7% paraformaldehyde for 10 min and then permeabilized using 0.1% Triton X-100 in PBS for 3 min. After being blocked with 1% BSA in PBST (0.05% Tween-20 in PBS) for 30 min, fixed cells were stained with primary antibodies for 1 h and washed three times using PBST. Secondary antibodies were added for 1 h, and then washed three times using PBST. Coverslips were visualized under DeltaVision deconvolution microscope.

For single cell migration, MDA-MB-231 cells were cultured in a glass-bottom culture dish (MatTek). During imaging, cells were maintained in CO_2-independent medium (Gibco) containing 10% FBS and 2 mM glutamine in a sealed chamber at 37°C. Images of living cells were taken with a DeltaVision microscopy system at 1 frame/10 min. Images were prepared for publication using Photoshop (Adobe).

For the wound-healing assay, confluent MDA-MB-231 and MDA-MB-468 cells transfected with the indicated siRNAs were scratched with a 10-μl pipette tip and then stimulated by CCL18 (20 ng/ml) or EGF (100 ng/ml) at 37°C for the indicated times. Images were taken with a 10× objective of an inverted microscope (Axiovert 200) coupled with an AxioCam-HS digital camera (Carl Zeiss). The relative healing velocities were measured using ImageJ software (National Institutes of Health).

In vitro acetylation assay

The acetylation reaction was performed essentially as described by Xia et al. (2012). Purified His-tagged wild-type and mutants of ACAP4 were incubated with GST-PACF-TC in 40 μl HAT buffer (20 mM Tris-HCl, pH 8.0, 10% glycerol, 100 mM NaCl, 1 mM DTT, 1 mM EDTA) containing 100 μM acetyl-CoA for 1 h at 30°C. After acetylated, samples were boiled in sample buffer and separated by SDS-PAGE and immunoblotted with either pan-acetylation antibody (pan acK) or site-specific acK311 antibody.

Identification of ACAP4 acetylation sites by mass spectrometry

To identify *in vivo* acetylation sites of ACAP4, MDA-MB-231 cells were transfected with FLAG-ACAP4. Twenty-four hours after transfection, cells were stimulated by 20 ng/ml CCL18 for 4 h. Cells were lysed in Tris-HCl buffer, and FLAG-ACAP4 was immunoprecipitated by FLAG M2 beads, boiled in sample buffer, and separated by SDS-PAGE. Bands corresponding to ACAP4 were

subjected to in-gel trypsin digestion. The labeled peptides were analyzed by LC–MS/MS with nano-LC combined with mass spectrometer as previously described (Zhao et al., 2013).

Liposome sedimentation and tubulation assay

Large unilamellar vesicles (LUVs) consisting of total brain lipids (Folch fraction 1; Sigma Chemicals) were resuspended in sedimentation buffer A (20 mM Hepes, pH 7.4, 150 mM NaCl, 1 mM EDTA, 1 mM DTT) and sized by extrusion to 100 μm. The sedimentation and tubulation assays were performed as previously described (Peter et al., 2004). For sedimentation assays, proteins were precentrifugated at 80000 rpm for 10 min and then incubated with liposomes in sedimentation buffer A for 20 min. Samples were centrifugated at 70000 rpm for 20 min. Supernatants and pellets were separated by SDS-PAGE. For tubulation assays, proteins were incubated with LUVs for 10 min, spread on glow-discharged carbon-coated grids, and negatively stained with 1% uranylacetate as previously described (Zhao et al., 2013).

Phospho-lipid binding ACAP4 in vitro

Echelon PIP strips containing 15 different biologically active lipids were purchased from Echelon (P-6001). Echelon PIP strips spotted with 15 different biologically active lipids were incubated with recombinant His-ACAP4^{WT}, His-ACAP4^{K311Q}, and His-ACAP4^{K311R} according to the manufacturer's instructions. Binding characteristics of acetylation-mimicking mutant ACAP4^{K311Q} and non-acetylatable mutant ACAP4^{K311R} on PIP strips were compared with those of the wild-type ACAP4.

Digitonin permeablization and subcellular redistribution assay

MDA-MB-231 cells transfected with WT or K311Q/R mutants of ACAP4 were permeabilized with 0.1% (*v/v*) digitonin in K buffer (20 mM Hepes, 10 mM Tris, pH 7.4, 100 mM KCl, 20 mM NaCl, 1.2 mM $MgSO_4$, 1 mM NaH_2PO_4, 40 mM mannitol) after 20 ng/ml CCL18 stimulation for 10 min as previously described (Ding et al., 2008). Cells were incubated with the K buffer at room temperature for 10 min before centrifugation at 200× *g* for 5 min. Supernatants and pellets were separated and analyzed by western blotting.

In some cases, aliquots of MDA-MB-231 cells were pretreated with C146 (2 μM) for 15 min prior to CCL18 stimulation (20 ng/ml) for 10 min. Treated cells were then collected and permeabilized with digitonin followed by separation of membrane and cytosol fractions as outlined above. Subsequently, equal amount (35 μg) of total membrane and cytosol proteins were applied for SDS-PAGE followed by western blotting analyses with anti-ACAP4, anti-actin, and anti-acK311 antibodies.

ARF6 GTPase pull-down assay

ARF6 in 293T cells were measured by pull-down its GTP-bound forms using GST-GGA3^{GAT} from various cell lysates as previously described (Santy and Casanova, 2001). The precipitated ARF6 was analyzed by western blotting using ARF6 antibody to compare with the level of total ARF6 proteins (both GTP-bound and GDP-bound).

Boyden chamber assay

MDA-MB-231 and MDA-MB-468 cells were transfected with WT or the K311Q/R mutants of ACAP4. Sixteen hours after transfection, cell suspension containing 1×10^5 cells/ml in serum-free media was prepared and 100 μl cell suspension was added into the Corning-Costar 3422 transwell chamber with 500 μl DMEM (10% FBS) in the lower wells. Then invasion assay was performed at 37°C for 16–24 h according to the manufacturer's instructions. Non-migratory cells were removed from the chamber using cotton-tipped swabs. Subsequently, the migrated cells through the chamber were fixed, stained with crystal violet, and counted.

Data analyses

To determine significant differences between means, unpaired Student's *t*-test assuming unequal variance was performed and evaluated using GraphPad Software (Mo et al., 2016). Statistical analysis was considered significant when the two-sided *P*-value was <0.05.

Supplementary material

Supplementary material is available at *Journal of Molecular Cell Biology* online.

Acknowledgements

We thank Fengrui Yang and Cathrine Rono for technical assistance and members of our groups for stimulating discussion.

Funding

This work was supported by the National Natural Science Foundation of China (31430054, 31621002, 31320103904, 81630080, 31671405, 31471275, and 31501130), the National Key Research and Development Program of China (2017YFA0503600, 2016YFA0100500, and 2016YFA0101202), the Ministry of Education (IRT_17R102, 20113402130010), the Strategic Priority Research Program of Chinese Academy of Sciences (XDB19000000), National Institutes of Health Grants (CA 164133, DK115812, and DK56292), and Central University Grants (WK2070000066).

Conflict of interest: none declared.

References

Bonecchi, R., Locati, M., and Mantovani, A. (2011). Chemokines and cancer: a fatal attraction. Cancer Cell *19*, 434–435.

Bowers, E.M., Yan, G., Mukherjee, C., et al. (2010). Virtual ligand screening of the p300/CBP histone acetyltransferase: identification of a selective small molecule inhibitor. Chem. Biol. *17*, 471–482.

Chen, J., Yao, Y., Gong, C., et al. (2011). CCL18 from tumor-associated macrophages promotes breast cancer metastasis via PITPNM3. Cancer Cell *19*, 541–555.

Condeelis, J., and Pollard, J.W. (2006). Macrophages: obligate partners for tumor cell migration, invasion, and metastasis. Cell *124*, 263–266.

Ding, X., Deng, H., Wang, D., et al. (2010). Phospho-regulated ACAP4-ezrin interaction is essential for histamine-stimulated parietal cell secretion. J. Biol. Chem. *285*, 18769–18780.

Ding, X., Wu, F., Guo, Z., et al. (2008). Molecular dissection of HCl secretion in gastric parietal cells using streptolysin O permeabilization. Methods Mol. Biol. *440*, 217–226.

Donaldson, J.G., and Jackson, C.L. (2011). ARF family G proteins and their regulators: roles in membrane transport, development and disease. Nat. Rev. Mol. Cell Biol. *12*, 362–375.

Du, D., Xu, F., Yu, L., et al. (2010). The tight junction protein, occludin, regulates the directional migration of epithelial cells. Dev. Cell *18*, 52–63.

D'Souza-Schorey, C., and Chavrier, P. (2006). ARF proteins: roles in membrane traffic and beyond. Nat. Rev. Mol. Cell Biol. *7*, 347–358.

D'Souza-Schorey, C., Li, G., Colombo, M.I., et al. (1995). A regulatory role for ARF6 in receptor-mediated endocytosis. Science *267*, 1175–1178.

Fang, Z., Miao, Y., Ding, X., et al. (2006). Proteomic identification and functional characterization of a novel ARF6 GTPase-activating protein, ACAP4. Mol. Cell. Proteomics *5*, 1437–1449.

Ghizzoni, M., Wu, J., Gao, T., et al. (2012). 6-alkylsalicylates are selective Tip60 inhibitors and target the acetyl-CoA binding site. Eur. J. Med. Chem. *47*, 337–344.

Gillingham, A.K., and Munro, S. (2007). The small G proteins of the Arf family and their regulators. Annu. Rev. Cell Dev. Biol. *23*, 579–611.

Ha, V.L., Bharti, S., Inoue, H., et al. (2008). ASAP3 is a focal adhesion-associated Arf GAP that functions in cell migration and invasion. J. Biol. Chem. *283*, 14915–14926.

Ismail, S.A., Vetter, I.R., Sot, B., et al. (2010). The structure of an Arf-ArfGAP complex reveals a Ca^{2+} regulatory mechanism. Cell *141*, 812–821.

Jaffe, A.B., and Hall, A. (2005). Rho GTPases: biochemistry and biology. Annu. Rev. Cell Dev. Biol. *21*, 247–269.

Jian, X., Tang, W.K., Zhai, P., et al. (2015). Molecular basis for cooperative binding of anionic phospholipids to the PH domain of the Arf GAP ASAP1. Structure *23*, 1977–1988.

Kim, T.H., Monsefi, N., Song, J.H., et al. (2015). Network-based identification of feedback modules that control RhoA activity and cell migration. J. Mol. Cell Biol. *7*, 242–252.

Kodelja, V., Muller, C., Politz, O., et al. (1998). Alternative macrophage activation-associated CC-chemokine-1, a novel structural homologue of macrophage inflammatory protein-1 alpha with a Th2-associated expression pattern. J. Immunol. *160*, 1411–1418.

Kolaczkowska, E., and Kubes, P. (2013). Neutrophil recruitment and function in health and inflammation. Nat. Rev. Immunol. *13*, 159–175.

Macia, E., Partisani, M., Favard, C., et al. (2008). The pleckstrin homology domain of the Arf6-specific exchange factor EFA6 localizes to the plasma membrane by interacting with phosphatidylinositol 4,5-bisphosphate and F-actin. J. Biol. Chem. *283*, 19836–19844.

Malaby, A.W., van den Berg, B., and Lambright, D.G. (2013). Structural basis for membrane recruitment and allosteric activation of cytohesin family Arf GTPase exchange factors. Proc. Natl Acad. Sci. USA *110*, 14213–14218.

Mo, F., Zhuang, X., Liu, X., et al. (2016). Acetylation of Aurora B by TIP60 ensures accurate chromosomal segregation. Nat. Chem. Biol. *12*, 226–232.

Nieto, M.A. (2013). Epithelial plasticity: a common theme in embryonic and cancer cells. Science *342*, 1234850.

Ouellette, M.H., Martin, E., Lacoste-Caron, G., et al. (2016). Spatial control of active CDC-42 during collective migration of hypodermal cells in Caenorhabditis elegans. J. Mol. Cell Biol. *8*, 313–327.

Pang, X., Fan, J., Zhang, Y., et al. (2014). A PH domain in ACAP1 possesses key features of the BAR domain in promoting membrane curvature. Dev. Cell *31*, 73–86.

Peter, B.J., Kent, H.M., Mills, I.G., et al. (2004). BAR domains as sensors of membrane curvature: the amphiphysin BAR structure. Science *303*, 495–499.

Peters, P.J., Hsu, V.W., Ooi, C.E., et al. (1995). Overexpression of wild-type and mutant ARF1 and ARF6: distinct perturbations of nonoverlapping membrane compartments. J. Cell Biol. *128*, 1003–1017.

Raman, D., Sobolik-Delmaire, T., and Richmond, A. (2011). Chemokines in health and disease. Exp. Cell Res. *317*, 575–589.

Rios Garcia, M., Steinbauer, B., Srivastava, K., et al. (2017). Acetyl-CoA carboxylase 1-dependent protein acetylation controls breast cancer metastasis and recurrence. Cell Metab. *26*, 842–855 e845.

Sakamoto, A., Tsukamoto, T., Furutani, Y., et al. (2016). Live-cell single-molecule imaging of the cytokine receptor MPL for analysis of dynamic dimerization. J. Mol. Cell Biol. *8*, 553–555.

Santy, L.C., and Casanova, J.E. (2001). Activation of ARF6 by ARNO stimulates epithelial cell migration through downstream activation of both Rac1 and phospholipase D. J. Cell Biol. *154*, 599–610.

Schafer, D.A., D'Souza-Schorey, C., and Cooper, J.A. (2000). Actin assembly at membranes controlled by ARF6. Traffic *1*, 892–903.

Sengupta, P., Jovanovic-Talisman, T., Skoko, D., et al. (2011). Probing protein heterogeneity in the plasma membrane using PALM and pair correlation analysis. Nat. Methods *8*, 969–975.

Shen, Y., Li, N., Wu, S., et al. (2008). Nudel binds Cdc42GAP to modulate Cdc42 activity at the leading edge of migrating cells. Dev. Cell *14*, 342–353.

Su, S., Liu, Q., Chen, J., et al. (2014). A positive feedback loop between mesenchymal-like cancer cells and macrophages is essential to breast cancer metastasis. Cancer Cell *25*, 605–620.

Tilston-Lünel, A.M., Haley, K.E., Schlecht, N.F., et al. (2016). Crumbs 3b promotes tight junctions in an ezrin-dependent manner in mammalian cells. J. Mol. Cell Biol. *8*, 439–455.

Valm, A.M., Cohen, S., Legant, W.R., et al. (2017). Applying systems-level spectral imaging and analysis to reveal the organelle interactome. Nature *546*, 162–167.

Xia, P., Liu, X., Wu, B., et al. (2014a). Superresolution imaging reveals structural features of EB1 in microtubule plus-end tracking. Mol. Biol. Cell *25*, 4166–4173.

Xia, P., Wang, Z., Liu, X., et al. (2012). EB1 acetylation by P300/CBP-associated factor (PCAF) ensures accurate kinetochore-microtubule interactions in mitosis. Proc. Natl Acad. Sci. USA *109*, 16564–16569.

Xia, P., Zhou, J., Song, X., et al. (2014b). Aurora A orchestrates entosis by regulating a dynamic MCAK-TIP150 interaction. J. Mol. Cell Biol. *6*, 240–254.

Yao, X., Anderson, K.L., and Cleveland, D.W. (1997). The microtubule-dependent motor centromere-associated protein E (CENP-E) is an integral component of kinetochore corona fibers that link centromeres to spindle microtubules. J. Cell Biol. *139*, 435–447.

Yu, X., Wang, F., Liu, H., et al. (2011). ACAP4 protein cooperates with Grb2 protein to orchestrate epidermal growth factor-stimulated integrin beta1 recycling in cell migration. J. Biol. Chem. *286*, 43735–43747.

Yuan, X., Yao, P.Y., Jiang, J., et al. (2017). MST4 kinase phosphorylates ACAP4 protein to orchestrate apical membrane remodeling during gastric acid secretion. J. Biol. Chem. *292*, 16174–16187.

Zhang, B., Yin, C., Li, H., et al. (2013). Nir1 promotes invasion of breast cancer cells by binding to chemokine (C-C motif) ligand 18 through the PI3K/Akt/GSK3beta/Snail signalling pathway. Eur. J. Cancer *49*, 3900–3913.

Zhao, X., Wang, D., Liu, X., et al. (2013). Phosphorylation of the Bin, Amphiphysin, and RSV161/167 (BAR) domain of ACAP4 regulates membrane tubulation. Proc. Natl Acad. Sci. USA *110*, 11023–11028.